IEEE Access
Multidisciplinary | Rapid Review | Open Access Journal

Received 29 December 2022, accepted 21 January 2023, date of publication 10 February 2023, date of current version 15 February 2023.

Digital Object Identifier 10.1109/ACCESS.2023.3244066

RESEARCH ARTICLE

Microstates of Dynamic Directed Connectivity Networks Revealing Visual Color Influences on the Brain Information Processing During Learning

MEEI TYNG CHAI[1,2], (Member, IEEE), AND TONG BOON TANG[1], (Senior Member, IEEE)
[1]Centre for Intelligent Signal and Imaging Research (CISIR), Institute of Health and Analytics, Universiti Teknologi PETRONAS, Seri Iskandar 32610, Malaysia
[2]Department of Computer Science, Faculty of Information and Communication Technology, Universiti Tunku Abdul Rahman, Kampar 31900, Malaysia

Corresponding author: Tong Boon Tang (tongboon.tang@utp.edu.my)

This work was supported in part by the Ministry of Higher Education (MOHE) Malaysia under the Higher Institution Centre of Excellence (HICoE) Program Fund to the Centre for Intelligent Signal and Imaging Research, Universiti Teknologi PETRONAS; and in part by Yayasan UTP under Grant 015LC0-234.

This work involved human subjects or animals in its research. Approval of all ethical and experimental procedures and protocols was granted by the Medical Research Ethics Committee of Royal College of Medicine Perak under Application No. UniKLRCMP/MREC/2018/009 and performed in line with the Declaration of Helsinki.

ABSTRACT Color has the exceptional ability to capture visual attention and is also capable of enhancing positive emotions, leading to a significant impact on human learning and memory. However, the influence of color on the spatiotemporal dynamics of brain connectivity networks during learning has remained unexplored. This study aimed to propose an analytical approach based on time-frequency decomposition and microstate analysis to capture temporal variations in dynamic directed connectivity networks using electroencephalography (EEG) signals for investigating the influence of visual color on network dynamics of the brain during a learning task. Wavelet transform and phase slope index were employed to estimate the dynamic directed connectivity networks of EEG signals. The estimated dynamic directed connectivity networks were then characterized using graph theoretical analysis. The recurring patterns of dynamic directed connectivity networks were classified using cluster analysis before the temporal dynamics of directed connectivity networks were quantified using microstate analysis. Forty-five healthy participants participated in the experiment, which included memorizing learning materials presented in three different colors (achromatic, cool, and warm). The results revealed that the dynamic directed connectivity networks could be grouped into several quasi-stable states and the presence of common and unique brain states repetitive across frequency bands under individual conditions. A joint analysis of all conditions revealed that the temporal dynamics (coverage, mean duration, and state transition probability) differed significantly between the achromatic and colored conditions. Few dynamic brain states were shared between conditions and tended to remain in particular brain states for a longer duration in specific frequency bands. Our observations provided the first evidence of temporal dynamics of frequency-specific directed connectivity networks in the brain during multimedia learning tasks, that is, increased coverage of top-down interactions in the θ and α bands and switching between top-down and bottom-up interactions (information flow from anterior to posterior regions and vice versa) in the α band, in colored conditions compared to that of achromatic conditions. Therefore, these results suggest that several frequency-specific directed connectivity networks cooperate during knowledge acquisition and may change over time (from one state to another). The proposed framework captures the temporal dynamics of directed connectivity networks, and provides implications for monitoring and assessing emotional and cognitive processes in various contexts.

INDEX TERMS Complex Morlet wavelet, directionality index, dynamic directed connectivity network, electroencephalography, k-means clustering, microstate analysis, phase slope index.

The associate editor coordinating the review of this manuscript and approving it for publication was Ludovico Minati.

This work is licensed under a Creative Commons Attribution 4.0 License. For more information, see https://creativecommons.org/licenses/by/4.0/

I. INTRODUCTION

Emotion is a crucial element for optimal learning and memory, because the learner's emotional state controls attention, which influences working memory and long-term memory processes (encoding, retention, and recall) [1]. In the multimedia learning context, positive emotions can be induced by applying emotional design principles in multimedia learning materials using appealing colors (yellow, orange, pink, green, blue, and purple) and round shapes (with anthropomorphisms). Studies have revealed that positive emotions improve learning performance (comprehension and immediate recall), intrinsic motivation, cognitive engagement, and satisfaction [2], [3], [4]. Moreover, it also creates a learning environment that promotes a positive perception toward the content and enables more engagement and interaction with the learning materials. To date, these studies have been limited to subjective measurements (self-reported emotional ratings) and behavioral-based assessment methods (paper-and-pen performance tests). While some researchers have explored eye-tracking [5], [6], [7] and heart rate variability [8], [9], both indirect measurements (quantifying ocular and heart responses make less inference to brain dynamics). We have limited knowledge of the effect of emotional design on information processing in the brain during learning. Hence, this study suggests the use of an objective and continuous measurement of brain dynamics (using a functional neuroimaging technique) for the assessment of the learning process with emotional design materials, because such method provides direct information about emotional and cognitive processing in the brain during learning, which can be a more accurate and reliable result of the experiment.

Electroencephalogram (EEG) is a most widely used functional neuroimaging technique for brain research in capturing dynamic connectivity networks owing to its distinct advantage—a superior temporal resolution that enables detection of fluctuations in brain interactions, in addition to being portable, non-invasive, and low-cost [10], [11]. Previously, we studied the effects of color on emotion, memory, and brain interactions in relation to emotional-cognitive processing, using EEG [12]. The interaction patterns were characterized using graph theoretical analysis [13]. Experimental results showed that (i) colored multimedia learning materials induce a positive emotional state on the learner, activate the brain to focus, and process information resulting in higher performance on memory recall tests (after 30-minutes and 1-month); (ii) the information flows in the brain are dependent on the color used in multimedia learning materials design, that is, the directionality indices showed long-range anterior-posterior connectivity from the prefrontal and frontal regions to posterior cortical regions in two EEG bands (theta and alpha bands). These results suggest that color significantly influences the direction of information flow, which is consistent with top-down processing when focused on external stimuli for optimized learning [14], and is indirectly linked with top-down attentional processes associated with working memory and emotional regulation processes [15], [16]. However, our previous study focused on the static representation of directed connectivity, which may overlook information about changes in brain-directed connectivity patterns over time.

Temporal dynamics of the direction of information flow in the brain during cognitive and emotional information processing have been shown to be necessary because brain interactions are inherently directed and dynamic [17], [18], and can be examined using a dynamic directed connectivity network analysis. Previous studies have reported the time-frequency analysis of dynamic directed connectivity performed through adaptive filters (Kalman filtering [19], recursive least square [20], and least mean squares [21]), which are *parametric approaches*. For example, the time-varying multivariate autoregressive (MVAR) approach has been proposed to model time-variant Granger causality [22] and partial directed coherence [23] using adaptive filters with coefficients that change with respect to time. However, the model order and dimensions must be determined before applying the MVAR model [24], [25]. The selection of an optimal model order can be challenging because of the variation in participants, experimental tasks, quality and complexity of the brain signals, number of channels, and model estimation techniques used [26]. Although some approximations have been suggested to help estimate the model order, such as the Akaike information criterion and Bayesian information criterion, the accuracy varies with the different MVAR models used. The classic method of capturing connectivity dynamics uses a sliding window [24], [25], in which the selection of the window length is required, and the signal of a short time window is assumed to be stationary. The accuracy of the estimation depends on the number of repetitions of the experimental conditions [26].

An alternative method to capture connectivity dynamics is via traditional model-free, *nonparametric approaches* such as short-time Fourier transform, wavelet transform, and Hilbert transform to overcome the constraints of parametric approaches [27]. Nonparametric approaches do not require selection of the window length (excluding short-time Fourier transform), model order, model dimension, etc. Nonparametric methods still require the initial selection of certain parameters. For instance, wavelet transform requires the selection of parameters (number of wavelet cycles and peak frequency) that regulate the trade-off between temporal and spectral resolution, and this affects the estimation of functional connectivity [28]. However, the selection of parameters in nonparametric methods is non-complex, and several recommendations are provided in the literature [28], [29].

Although many studies have applied wavelet transform to EEG data, they have utilized power and phase information to measure either power spectral density [30] or functional connectivity [31], [32], [33], which are not able to capture the direction of information flow between brain regions (for a deeper understanding of brain dynamics). The power and

phase information obtained from wavelet transform analysis can be further exploited to study information flow (directed connectivity network) in the brain over time. Thus, the result is a sequence of non-overlapping brain states (only one dominant state presents at a time), so-called microstates, that can be analyzed using microstate analysis. Microstate analysis considers multichannel EEG data as a sequence of discrete brain states/microstates visualized as topographical maps remaining stable for a short time before transitioning into another state. The occurrence of similar maps repeats over time [34], and changes in microstate are measured by temporal parameters, including mean duration, coverage, and state transition probability [35]. Previous microstate studies have focused on brain functional connectivity networks during visual oddball tasks [36], mental calculation [31], mental fatigue [37], and resting states [38], [39]. To the best of our knowledge, there has been no published microstate analysis of the effect of color on the temporal dynamics of frequency-specific directed connectivity during the learning process. Tracking directed connectivity dynamics in the brain during the learning process can provide insights into significant changes in directed connectivity patterns and a better understanding of how the brain processes information. Therefore, a data-driven approach for investigating the temporal dynamics of brain activity during a learning task, based on dynamic directed connectivity analysis and microstate analysis using EEG, is a novel method.

This study investigated the temporal dynamics of frequency-specific directed connectivity networks induced by visual color during a learning task, using EEG. This work combines three major techniques:1) wavelet-based time-frequency decomposition with a phase slope index [40] was used to extract the time-varying EEG features for dynamic directed connectivity estimation (time and frequency domains); 2) graph theoretical analysis was used to characterize the patterns of directed connectivity networks prior to the cluster analysis, which was used to identify recurring patterns of directed connectivity networks; and 3) the microstate approach was used to capture the temporal dynamics of directed connectivity networks in the brain. We hypothesized that different visual colors (achromatic/cool/warm colors) affect information processing differently during learning, and the effects could be detected from directed connectivity network patterns (i.e., topographical maps) and dynamics (how the directed connectivity networks change over time).

The remainder of this study is organized as follows. In Section II, the participants and experimental protocol, EEG data acquisition and preprocessing, proposed wavelet-based phase slope index approach for estimating dynamic directed connectivity networks, graph theoretical analysis for characterizing patterns of directed connectivity networks, and clustering analysis for identifying recurring patterns of directed connectivity networks are described in detail. The results of the proposed method are presented in Section III, and a discussion of the results and limitations are presented in Sections IV and V, respectively. Finally, Section VI concludes the paper.

II. MATERIALS AND METHODS

A. PARTICIPANTS AND EXPERIMENTAL PROTOCOL

The EEG data were collected from a group of 45 healthy young adults (18-24 years of age: mean 20.12 ($\pm$0.47)) while they performed experimental tasks in our previous study [12]. All participants were right-handed, had normal or corrected-to-normal vision and normal color vision, had low prior knowledge, and were homogeneous cross groups (more detailed information is included in Supplementary Materials, Section I). The entire experiment comprised resting-state with eyes open, learning, self-emotional rating, and memory tasks (30-min recall and 1-month recall phases), as shown in Fig. 1. However, only continuous EEG signals during the learning task were analyzed in this study by investigating the color-related changes in the microstates of the dynamic directed connectivity network. During the learning task, participants learned and memorized the contents of multimedia learning materials without taking notes, and were informed that they would be tested to measure the retention of the learned contents. Visual illustrations of multimedia learning materials were displayed in achromatic colors for the control group (Condition 1: GB&W), cool colors for case condition #1 (Condition 2: CCI), and warm colors for case condition #2 (Condition 3: WCI). Note-taking was not allowed because it would i) require deeper processing, ii) interfere with visual information processing, iii) require more cognitive effort and time than reading alone, and iv) cause motion artifacts, all of which would likely alter EEG signals (for further discussion, refer [12]). The total length of the learning data was approximately 10.5 min for each participant.

The study protocol was approved by the Medical Research Ethics Committee of the Royal College of Medicine Perak (UniKLRCMP/MREC/2018/009). All subjects provided consent, and the study was conducted in accordance with the Declaration of Helsinki.

B. EEG DATA ACQUISITION

Data were obtained from EEG recordings during a multimedia learning task using eegosports amplifier (ANT Neuro, Enschede, Netherlands) with 32 gel-based Ag/Ag-Cl electrodes mounted on an EEG head cap. Electrode placements were based on the Extended International 10−20 system (10% system). All electrodes were referenced to CPz and grounded at AFz, according to the manufacturer's recommendations (eemagine Medical Imaging Solutions GmbH, Berlin, Germany). The readings of the electrode impedance were all maintained at $<$10 kΩ and sampled at 2048 Hz throughout the recording sessions.

C. EEG PRE-PROCESSING AND CURRENT SOURCE DENSITY

EEG pre-processing was performed following the procedure described in [12]. Raw EEG signals were preprocessed

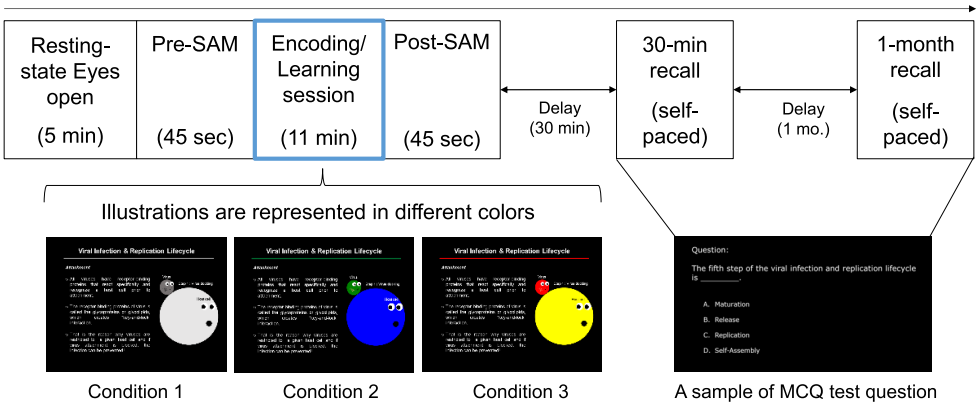

FIGURE 1. Experimental protocol and stimuli. The sequence of task sessions (top), the three versions of multimedia learning materials for the learning task (bottom) [achromatic-colored illustrations (Condition 1: GB&W); cool-colored illustrations (Condition 2: CCI); and warm-colored illustrations (Condition 3: WCI)], and a sample of test questions for the memory recall tests. Only the EEG signals during the learning task (blue box) were analyzed in the present work by investigating the colored-related changes in the microstates of dynamic directed connectivity networks. Adapted from [12].

offline to remove unwanted artifacts using BESA Research 6.0 (Besa GmbH, Gräfelfing, Germany). Data with voltage amplitudes exceeding $\pm 100\ \mu$V were rejected manually [41]. Artifact-corrected data were then transformed into the current source density (CSD) via the surface Laplacian method, which computes the second spatial derivative of the voltage at neighboring electrode sites using a spherical spline algorithm [42], [43]. The CSD transformation helps highlight local electrical activity by diminishing any representation of distal activity to determine brain connectivity at the sensor level (for further discussion, refer [12]). Finally, the corrected CSD-transformed EEG data were exported for further analyses using custom-made scripts and open-source toolboxes in MATLAB (MathWorks, Inc., Natick, MA). The open-source toolboxes included— the (1) Brain Connectivity Toolbox [13] for graph theoretical analysis and (2) EEGLAB [44] for topographical map plotting.

D. TIME-FREQUENCY ANALYSIS

The time-frequency decomposition was performed by convolving CSD-transformed signals with a family of complex Morlet wavelets (CMW) [45] to obtain both the time and frequency features of EEG. The CMW is defined as a Gaussian-windowed complex sine wave, as follows:

$$CMW = e^{i2\pi f_c t} e^{-t^2/2\sigma^2} \tag{1}$$

where i is the complex operator ($i = \sqrt{-1}$), t is the time in seconds (s), f_c is the peak frequency in hertz (Hz, i.e., peak frequency and central frequency are used interchangeably), which is increased from 1 to 60 Hz in 35 logarithmically spaced steps, and σ defines the width of the Gaussian in each frequency band, which is set to ($\sigma = s/2\pi f_c$) as s increases from 3 to 10 cycles over the 35 frequencies. Each member of the wavelet family was convolved with the EEG data to yield a separate time series of complex wavelet coefficients for each frequency, which are then used to extract power and phase information. A full spectral density matrix of the multivariate system (containing auto-spectral and cross-spectral densities) was derived from time–frequency decomposition via complex Morlet wavelet convolution in the frequency domain. The canonical EEG frequency bands of interest were selected for analysis: delta (δ:1–4 Hz), theta (θ:4–8 Hz), alpha (α:8–13 Hz), beta (β: 13–30 Hz), and gamma (γ:30–48 Hz). These are commonly used in electrophysiological research related to learning and memory [46]. In addition, information flow between different brain regions at different frequencies is associated with cognitive processes [47], [48], and brain connectivity networks are transient and dynamic [31], [36]. Thus, if the data are spatially, temporally, and spectrally resolved (by analyzing the brain networks as a function of frequency over time), it can provide more detailed information for capturing the brain dynamics of cognitive and emotional processes during learning.

E. DYNAMIC DIRECTED CONNECTIVITY NETWORK ESTIMATION

Directed connectivity networks are referred to as dynamic directed connectivity networks derived from the wavelet-based phase slope index (PSI). Briefly, it involves a three-step procedure: (i) compute the auto-spectral and cross-spectral densities of the signals obtained from the CMW convolution over time-frequency points, (ii) compute the complex coherency between signals, and (iii) estimate the dynamic PSI derived from the wavelet-decomposed EEG signals, which is described in detail in the subsequent paragraphs and summarized in Fig. 2.

In the first step, (time-dependent) auto-spectral and cross-spectral densities were computed. The autospectral density at one brain site (signal A), also called the power spectrum of

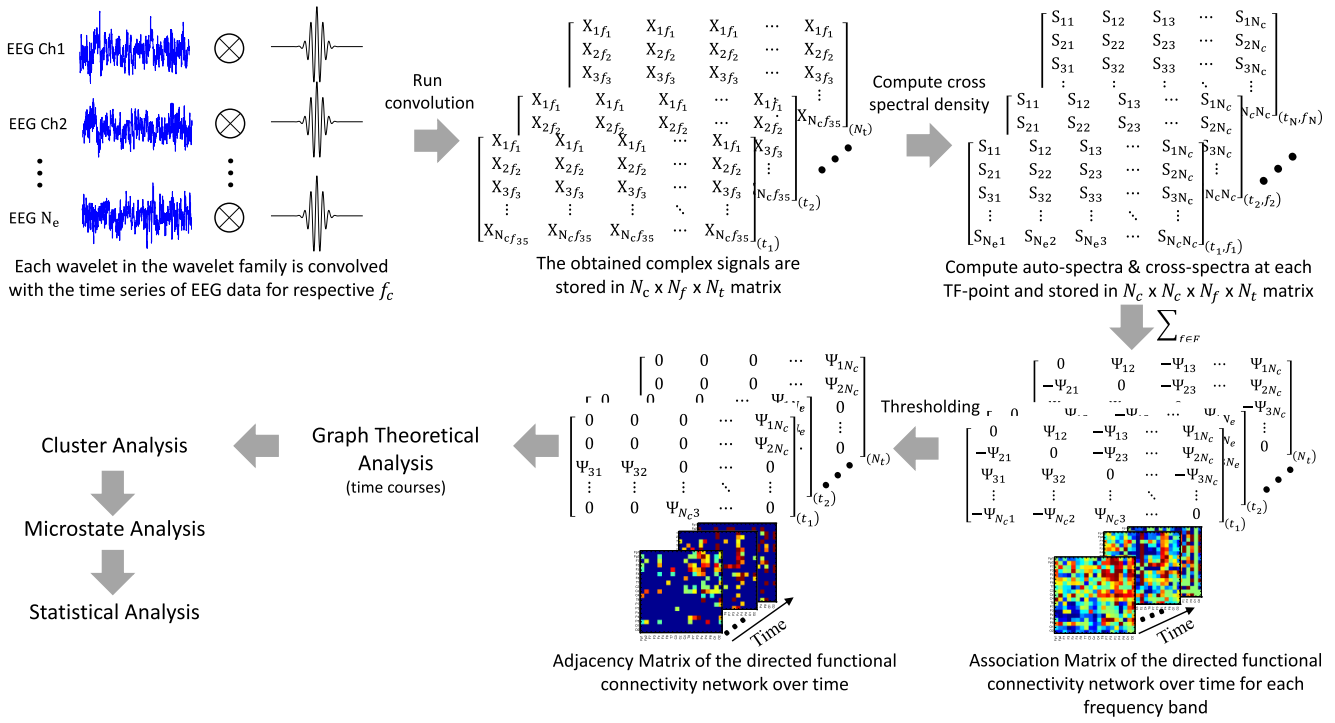

FIGURE 2. Flowchart for the proposed analytical method named wavelet-based PSI with cluster and microstate analyses for analyzing dynamic directed connectivity network. First, the time-frequency decomposition was carried out with CMW. The dynamics of the spectral densities and the phase slope of brain activity (directed connectivity networks) were then estimated. A statistical threshold ($\Psi > |2|$, $p < 0.05$) was applied to the directed connectivity network (association matrix) as in [40]. After thresholding, a time series of adjacency matrices are obtained, and then, its topological attributes (i.e., in- and out-degree) are extracted, which gives a measure of the directionality index over time. The cluster analysis was used to identify recurring patterns of directed connectivity networks in the joint time-frequency domain, and the microstate analysis was used to capture the temporal dynamics of directed connectivity networks.

A (P_A), can be expressed as follows:

$$S_{AA}(f,t) = P_A(f,t) = \langle S_A(f,t)\, S_A^*(f,t)\rangle \tag{2}$$

A similar equation to (2) was used to compute the auto-spectral density for the remaining signals. This yields a real number (the squared magnitude) using the product of a complex number and its conjugate. The cross-spectral density is defined as the expected value of the product of signal A and the complex conjugate of signal B, as shown in (3).

$$S_{AB}(f,t) = \langle S_A(f,t)\, S_B^*(f,t)\rangle \tag{3}$$

where $*$ denotes a complex conjugate $\langle . \rangle$ is the expectation value, $S_A(f,t)$ and $S_B(f,t)$ are the wavelet-decomposed EEG signals from brain regions A and B, respectively. Unlike auto-spectral density, cross-spectral densities are complex numbers.

In the second step, the complex coherency between any two signals A and B (Coh_{AB}) was computed by dividing the cross-spectrum with the square root of the product of the auto-spectrum of A (S_{AA}) and auto-spectrum of B (S_{BB}). Mathematically, the complex coherency [49] is expressed as

$$Coh_{AB}(f,t) = \frac{S_{AB}(f,t)}{\sqrt{S_{AA}(f,t)\, S_{BB}(f,t)}} \tag{4}$$

where S_{AA} and S_{BB} are real numbers, S_{AB} is a complex number, Coh_{AB} is complex-valued coherency.

In the final step, the PSI value [40] was estimated from the complex coherency to capture the causal influence between the multichannel signals. When the propagation speed was constant, the phase difference between A and B increased with frequency. Hence, the phase spectrum was expected to have a positive slope if A drove B ($A \rightarrow B$), and a negative slope if B drove A ($B \rightarrow A$). The change in the phase difference between the neighboring frequency bins of the complex coherency is computed to obtain the PSI for the desired frequency bands. The PSI estimates the dynamic slope of the phase difference as a function of frequency at each time point, which can be expressed as follows:

$$\tilde{\Psi}_{AB}(t) = \Im\left(\sum_{f\in F} Coh_{AB}^*(f,t)\, Coh_{AB}(f+\delta f,t)\right) \tag{5}$$

where Coh_{AB} is the complex coherency, $\Im$ is the imaginary part (i.e., the multiple of i; for example, if the estimated PSI is a + bi, the value of the imaginary part is b), δf is the incremental step in the frequency domain (depending on its corresponding range), and F is the set of frequencies over which the slope is summed ($F = \{\delta, \theta, \alpha, \beta, \gamma\}$, the five specific frequency bands defined in Section II-D). Considering the δ band, F satisfies 1 Hz $\leq f \leq$ 4 Hz, and the phase slope of signals between 1 and 4 Hz can

then be estimated. The same procedure was repeated for the remaining four frequency bands.

As the PSI was computed between pairs of EEG channels, the estimated PSIs were stored in an $N_c \times N_c$ matrix, which is equivalent to 171 possible pairwise associations ($(N_c^2 - N_c)/2$, where N_c =19 is the number of EEG channels: FP1, FP2, F7, F3, Fz, F4, F8, T7, C3, Cz, C4, T8, P7, P3, Pz, P4, P8, O1, and O2), and the diagonal was set to zero so that only cross-correlation rather than autocorrelation between EEG signals were considered for directed connectivity networks. The estimated PSI between signals A and B, $\tilde{\Psi}_{AB}$ at time t for each frequency band was stored in the form of an off-diagonal, skew-symmetric matrix, as follows:

$$\tilde{\Psi}_{AB}(t) = \begin{bmatrix} 0 & \tilde{\Psi}_{12} & -\tilde{\Psi}_{13} & \cdots & \tilde{\Psi}_{1N_c} \\ -\tilde{\Psi}_{21} & 0 & -\tilde{\Psi}_{23} & \cdots & \tilde{\Psi}_{2N_c} \\ \tilde{\Psi}_{31} & \tilde{\Psi}_{32} & 0 & \cdots & -\tilde{\Psi}_{3N_c} \\ \vdots & \vdots & \vdots & \ddots & \vdots \\ -\tilde{\Psi}_{N_c1} & -\tilde{\Psi}_{N_c2} & \tilde{\Psi}_{N_c3} & \cdots & 0 \end{bmatrix} \tag{6}$$

By randomly shuffling the PSI value over frequency bins 2000 times, the estimated outputs of PSI were normalized against null distributions to correct for any spurious results, where the t-statistic of the connectivity was compared with the generated null distribution of equivalent parameters estimated in random matrices containing the same number of nodes, connections, and connectivity degrees. Normalization was used to determine the significant value of PSI (as permutation testing is an appropriate statistical test as suggested by [50], [51] to deal with multiple comparisons) by subtracting the mean of the null distribution (μ_{null}) and then dividing by the standard deviation of that distribution (σ_{null}) as follows:

$$\Psi_{AB}(t) = \frac{\tilde{\Psi}_{AB}(t) - \mu_{null}(t)}{\sigma_{null}(t)} \tag{7}$$

After permutation testing, the normalized PSI values (Ψ) were evaluated at a significance level. The significant value of |2| where PSI distribution corresponded to 95% confidence interval of $p < 0.05$ (two-tailed test) was applied to the association matrix as in [40]. All subthreshold connectivity values ($\Psi < |2|$) were set to zero, and the suprathreshold connectivity values ($\Psi > |2|$) retained their original values. Finally, the time series of the adjacency matrix (the connection matrix that indicates the number of significant links between nodes in a network) was generated for each participant and every EEG frequency band. The topographical properties of the adjacency matrix (time courses) were quantified using graph theoretical analysis.

F. CHARACTERIZATION OF DYNAMIC DIRECTED CONNECTIVITY NETWORKS

Graph theoretical analysis quantifies topographical connectivity patterns, and it can be applied to brain connectivity networks [50]. The node degree was first computed prior to the computation of the directionality index over time. The degree of a node i was defined as the number of links connected to that node, which was determined from the time series of adjacency matrices. Since an adjacency matrix generated from PSI values show the direction of the information flow (directed network), a node's degree was computed by dividing it into *in*-degree and *out*-degree. The *in*-degree (k_i^{in}) denotes the number of incoming flows, and the *out*-degree (k_i^{out}) represents the number of outgoing flows [13] at each time point, which can be expressed as follows:

$$k_i^{in}(t) = \sum_{j \in N_c} A_{ji}(t) \tag{8}$$

$$k_i^{out}(t) = \sum_{j \in N_c} A_{ij}(t) \tag{9}$$

where A_{ij} is not necessarily equal to A_{ji} and represents the entry of the adjacency matrix. A node with a high *out*-degree value indicates that the region can influence others. Similarly, a node with a high *in*-degree value indicates that an area could be influenced by other regions.

Next, the directionality index (DI), which indicates the direction of information flow for each frequency band, was obtained by computing the difference between *out*-degree and *in*-degree vectors, as expressed by

$$DI_i(t) = \sum k_i^{out}(t) - \sum k_i^{in}(t) \tag{10}$$

A positive DI value indicates that the EEG channel behaves like a source/sender, whereas a negative DI value indicates a sink/receiver. Each directionality index of the directed connectivity network at time point $t(t = 1, 2 \ldots N_T)$ was stored in a row vector $V_t : 1 \times N_c$ and resulting in a feature matrix of $N_T \times N_c$ (for each frequency band), where N_T =6300 and N_c =19. This feature matrix was used as the input data for cluster analysis.

G. CLUSTER ANALYSIS

Cluster analysis was used to capture recurring patterns of directed connectivity networks in the joint time-frequency domain. The assumption was that patterns of directed connectivity networks may reoccur at both time and frequency. The cluster analysis was based on a data-driven (unsupervised) approach—K-means clustering [52] to partition the N_T-observations of the feature matrix into mutually exclusive K clusters ($K \ll N_T$) according to the measured distance so that each observation could be grouped into the most similar cluster, where rows and columns of the feature matrix corresponded to observations and EEG channels, respectively. Each observation belonged to only one state at a time (nonoverlapping clusters). In other words, each pattern of the directed connectivity network was assigned an index of its closest cluster. This produces a time series of the corresponding cluster indices for each participant and EEG frequency band. The initial parameters for k-means clustering analysis were predefined as follows: The number

of clusters is set as $K = 16$. This was selected based on the explained variance [35], which was computed as a function of the number of clusters (with a search range of 2−20 and explained variance cut-off at >0.90≡90%). These 16 clusters accounted for 92.6% of the total variance in EEG data. The simulations for 16 initial centroid positions were selected from the feature matrix at random (*kmeans* implements the k-means++ algorithm by default), and the k-means algorithm was repeated 500 times with a new initial cluster centroid on the same data to find the best cluster centroids for each of the datasets [33], [38], where the best cluster centroids represent the final centroid locations — 1) with the minimum within-cluster sum of point-to-centroid distances (*sumd*) among all the re-runs/replicates, 2) when the centroids of newly generated clusters were no longer changing, or 3) when the maximum number of iterations was reached. The maximum number of iterations (*MaxIter*) was set to 1,000 for solution convergence and computation time efficiency. On average, the algorithm required less than 250 iterations for convergence in all 500 reruns.

Two cluster analyses were performed. For the first cluster analysis, recurring patterns of directed connectivity networks in the joint time-frequency domain for each condition were determined separately by concatenating $N_T \times N_c$ matrix along the five frequency bands, which eventually provided a specific set of topographical maps corresponding to each condition: GB&W, CCI, and WCI. Pearson's correlation analysis was performed to investigate the correlation between topographical connectivity patterns and topographical maps that were unique to a particular experimental condition.

For the second cluster analysis, the temporal dynamics of the common patterns of directed connectivity networks shared between conditions were determined and compared by concatenating the $N_T \times N_c$ matrix with frequencies, subjects, and conditions. The term brain state refers to the recurring patterns of the directed connectivity networks identified in the cluster analysis as analogous to that of microstates, which can be analyzed using microstate analysis.

H. DYNAMIC STATE COMPUTATION (MICROSTATE ANALYSIS)

Following the cluster analyses, the temporal parameters of coverage, mean duration, and state transition probability were evaluated for each of the 16 identified states.

Coverage (*Cov*) is the percentage of time covered by a given state [35], which can be represented by

$$Cov(\%) = (n_d / n_o) \times 100 \tag{11}$$

where n_d is the number of times a state is dominant and n_o is the total number of observations.

Mean duration (MD) is the amount of time the brain stays at a particular state or the average time in milliseconds (ms) covered by a given state [35], which can be expressed as

$$MD(\text{ms}) = \sum n_l \Big/ n_t \tag{12}$$

where n_l is the length of time a microstate remains stable and n_t is the total time.

The state transition probability (STP) is the probability of switching between different states and is represented in the matrix form of $K \times K$ (i.e., state × states). The MATLAB implementation steps of the wavelet-based PSI with cluster and microstate analyses are summarized in Algorithm 1.

Algorithm 1 Wavelet-Based PSI With Cluster and Microstate Analyses

Input: Multichannel EEG signals, $x_i(t)$, where $i = 1, 2, \ldots, N_c$
Output: Network measures X_{norm}, Cov, MD & STP
Step 1: Complex Morlet wavelet convolution
- Define x-, y- and z-coordinates for the 19 electrodes
- Compute the CSD using the function laplacian_perrinX.m
- Create the CMW using (1)
- Convolute CMW with the $x_i(t)$

Step 2: Dynamic directed connectivity network estimation
- Compute the $S_{AA}(f,t)$ and $S_{BB}(f,t)$ using (2)
- Compute the cross-spectral matrix $S_{AB}(f,t)$ using (3)
- Compute the complex coherency $Coh_{AB}(f,t)$ using (4)
- Compute the wavelet-based PSI $\tilde{\Psi}_{AB}(t)$ using (5)

Step 3: (dynamic) Graph theoretical analysis
- Perform the 2000 permutations of directed connectivity matrices
- Compute the normalized wavelet-based PSI $\Psi(t)$ using (7)
- Extract the *in*-degree (k_i^{in}) using (8)
- Extract the *out*-degree (k_i^{out}) using (9)
- Compute the directionality index (DI_i) using (10)
- Perform the 2000 permutations of random networks (using Brain Connectivity Toolbox function "randmio_dir")
- Compute normalized network measures X_{norm} using (13)

Step 4: Cluster analysis and dynamic state computation
- Perform k-means clustering
- Compute the coverage (Cov) using (11)
- Compute the mean duration (MD) using (12)
- Compute the state transition probability (STP) using HMM

I. STATISTICAL ANALYSIS

In the network analysis, the computed k_i^{in}, k_i^{out} and DI_i were normalized by random networks, which resulted from randomization of the corresponding directed connectivity matrices [50], [51]. Permutation testing has been widely used in EEG connectivity analysis as it helps reduce the would-be false-positive results (also known as Type 1 error) and allows multiple comparisons, that is, the multichannel time series of directed networks (a similar approach used in [36], [53], [54]). Randomization was repeated for 2000 permutations. At each permutation, a random network was generated from the estimated directed connectivity network. The connections of the directed connectivity network were randomly rewired, while preserving the *in*-degree and *out*-degree distributions. The normalized network measure X_{norm} is obtained as follows:

$$X_{norm} = \frac{X_{network}}{\langle X_{random} \rangle} \tag{13}$$

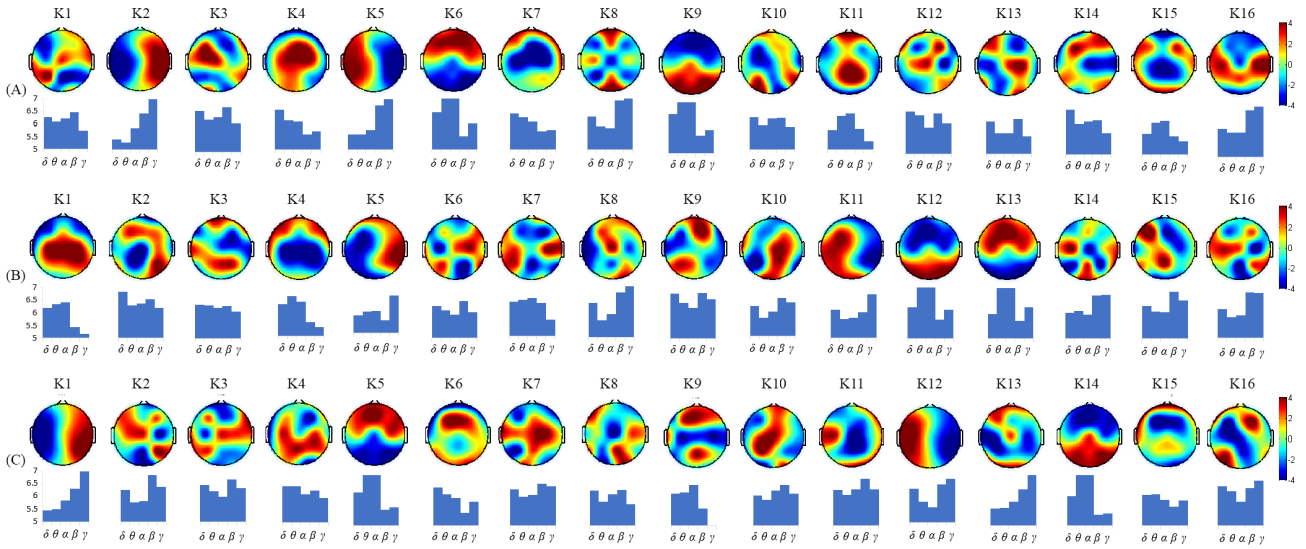

FIGURE 3. Topographical maps of the 16 brain states and their corresponding frequency histograms for (A) GB&W, (B) CCI, and (C) WCI conditions. The color map was set in the interval [−4, 4] and represents the flow of information (warm colors represent drivers, whereas cool colors represent recipients). Histograms illustrate the mean frequency of the coverage across frequencies (x-axis denotes the five bins of EEG frequency bands (δ, θ, α, β, γ) and y-axis denotes the number of occurrences set in the interval [5], [7]).

where $X_{network}$ is the computed network properties of directed connectivity (k_i^{in}, k_i^{out} and DI_i), and $\langle X_{random} \rangle$ is the average of 2000 random network properties.

The second step was to compare the differences in temporal parameters between frequency bands with respect to clusters based on (1) individual conditions (GB&W, CCI, and WCI) and (2) between conditions (GB&W vs. CCI vs. WCI). Two statistical tests were performed. First, the coverage of the clusters was calculated for each EEG frequency band, which was separated into five conditions, with each condition representing one EEG band. One-way repeated-measures analysis of variance with the EEG frequency bands (δ, θ, α, β, and γ) as within-participant factors was used to determine whether there was a significant difference in *Cov* between frequency bands for each condition. When comparing the differences in cluster coverage between bands with respect to clusters of the conditions, Bonferroni post-hoc tests were run on ten different combinations of the five frequency bands (${}^nC_r$ combinations, where $n = 5$ and $r = 2$). To minimize the risk of type-I errors, Bonferroni adjustment was made for multiple comparisons, resulting in a new significance level of $0.05/10 = 0.005$ ($p < 0.005$). Second, a one-way multivariate analysis of variance (MANOVA) and Tukey's HSD post-hoc test for multiple comparisons ($p < 0.05$) were conducted to determine significant differences between the conditions for the *Cov* and STP of the clusters on the five frequency bands. A nonparametric Kruskal-Wallis H test was performed because MD data were not distributed normally, followed by Mann-Whitney U post-hoc tests ($p < 0.05$) to determine statistically significant differences between conditions. All statistical analyses were performed using the software packages—MATLAB (MathWorks Inc., Natick, MA) and SPSS Statistics version 23 (IBM, Armonk, NY).

III. RESULTS

The experimental results are presented in this section. They are divided into two main parts. The first part examined the recurring patterns of directed connectivity networks across frequency bands that corresponded to each condition individually, which was obtained by the first cluster analysis. The second part examined the repeated patterns of directed connectivity networks across frequency bands that were shared among all participants, which was obtained from the second cluster analysis.

A. RECURRING PATTERNS OF DIRECTED CONNECTIVITY NETWORK ACROSS FREQUENCIES AT THE INDIVIDUAL CONDITION

The reoccurrences of the directed connectivity network across frequency bands corresponding to the GB&W, CCI, and WCI conditions, in the form of topographical maps together with their frequency histograms, are presented in Fig. 3(A)–(C), respectively. Topographical maps are the identified recurring patterns of directed connectivity networks represented by the centroids of k-means clusters. The histogram of the coverage of microstates indicates the EEG frequency bands at which a brain state tends to recur (so-called dominant/frequently occurring states). Certain brain states are seen to be more dominant than others at specific frequency bands. The results showed a higher percentage of coverage (>5%) than the average value, as summarized in Table 1. There was more than one dominant state in each frequency band (except for the delta band of the WCI condition). This demonstrates the dynamics of multiple-directed connectivity during a learning task. In addition, the dominant states were shared by more than one frequency band that was mostly found between θ

TABLE 1. Dominant states of the directed connectivity network at five frequency bands (δ, θ, α, β, γ) during each of the GB&W, CCI, and WCI conditions.

Conditions	Dominant states (Sorted from highest to lowest at the percentage of average > 5%)				
	Frequency bands				
	Delta, δ	*Theta, θ*	*Alpha, α*	*Beta, β*	*Gamma, γ*
GB&W	K14, K12, K3, K4	**K9**, **K6**	**K9**, **K6**	**K8**, **K16**, **K5**, K3, K12	**K5**, K2, **K8**, **K16**
CCI	K2, K9	**K13**, **K12**, K4	**K13**, **K12**, K1, K7	**K15**, **K16**, K9, **K8**, **K14**	**K8**, **K16**, K11, **K14**, **K15**
WCI	**K16**	**K5**, **K14**	**K5**, **K14**	K2, K11, K3, **K13**, K7, **K12**	K1, **K13**, **K12**, **K16**

1: Predominant states are labeled as "K#" where "K" stands for brain states; "#" denotes the assigned cluster index (1 to 16) resulted from the cluster analysis. The assigned number *varies* between conditions, see Fig. 3.
2: Predominant states in BOLD font means that the state is shared between two frequency bands.

and α bands or between β and γ bands. This finding was the first to demonstrate the temporal dynamics of directed connectivity patterns at five canonical EEG frequency bands and highlight the color-induced differences in directed connectivity patterns during a learning task using EEG microstate analysis.

In addition, the results of the correlation analysis for topographical connectivity patterns between conditions showed that few directed connectivity network maps had a strong correlation ($r > 0.7$) depending on the selected conditions for the analysis, indicating the similarity of directed connectivity networks between conditions. This indicates that there are common brain states among the three conditions. The results are as follows.

1) Two maps between GB&W and CCI were strongly correlated, GB&W K6 with CCI K13 ($r = 0.9060$) and GB&W K9 with CCI K12 ($r = 0.9190$).
2) The five maps between GB&W and WCI were strongly correlated: GB&W K2 with WCI K1 ($r = 0.9550$), GB&W K5 with WCI K12 ($r = 0.9426$), GB&W K6 with WCI K5 ($r = 0.9711$), GB&W K9 with WCI K14 ($r = 0.9768$), and GB&W K10 with WCI K16 ($r = 0.7570$).
3) Seven maps between CCI and WCI were strongly correlated: CCI K5 with WCI K1 ($r = 0.740$), CCI K6 with WCI K3 ($r = 0.7125$), CCI K10 with WCI K7 ($r = 0.7074$), CCI K11 with WCI K12 ($r = 0.8047$), CCI K12 with WCI K14 ($r = 0.9378$), CCI K13 with WCI K5 ($r = 0.9319$), and CCI K16 with WCI K2 ($r = 0.7969$).

Conversely, the correlation analysis results also demonstrated that some brain states had no significant correlation between the conditions, indicating that they are unique connectivity patterns for a particular condition. The identified brain states (common and unique directed connectivity patterns) could only be identified using a joint time-frequency analysis, where the temporal dynamics of the connectivity patterns could be assessed at different frequency bands. If directed connectivity is estimated by averaging the connectivity maps over the entire EEG recording time, the changes in connectivity patterns between brain regions might be wiped off. Therefore, a dynamic analysis of the information flow between different brain regions must be monitored for the cognitive and emotional information processing that gives rise to our behavior.

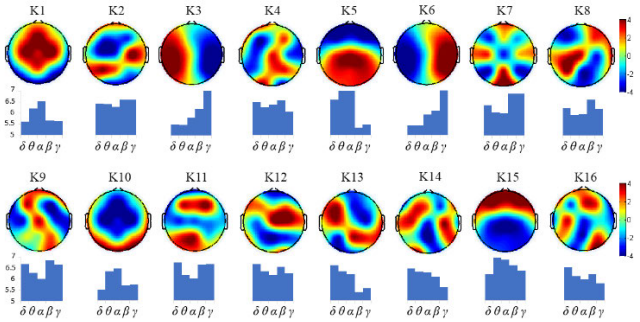

FIGURE 4. The 16 topographical maps of directed connectivity networks shared by all participants, with color map set in the interval [−4, 4]; Histograms illustrate the mean frequency profiles of the coverage (x-axis denotes the five bins of EEG frequency bands (δ, θ, α, β, γ) and y-axis denotes the number of occurrences set in the interval [5], [7]).

Next, the microstate features (including coverage, mean duration, and STP) were extracted, and differences between five frequency bands for the 16 states at each condition were statistically assessed using statistical tests, as described in Section II. Post-hoc tests revealed statistically significant differences in coverage and mean duration between the five frequency bands. A significant increase in coverage of long-range anterior-posterior connectivity from the prefrontal and frontal regions to the posterior cortical regions and vice versa (from posterior to anterior connectivity) was found in the θ and α bands for all conditions, and the increased coverage of short-range connectivity (within anterior regions, within posterior regions, and information flow from left to right hemisphere) was observed in the δ band and higher frequency bands (β and γ). Moreover, the overall mean duration of the microstates was longer in the lower frequency bands (δ and θ bands) than in the higher frequency bands (α, β and γ bands) for all conditions. The trends of all significant differences in the mean coverage between frequency bands are presented in Supplementary Tables 1–3. Similarly, the mean duration differences between the five frequency bands for the 16 states under each condition are shown in Supplementary Figs. S1-S3.

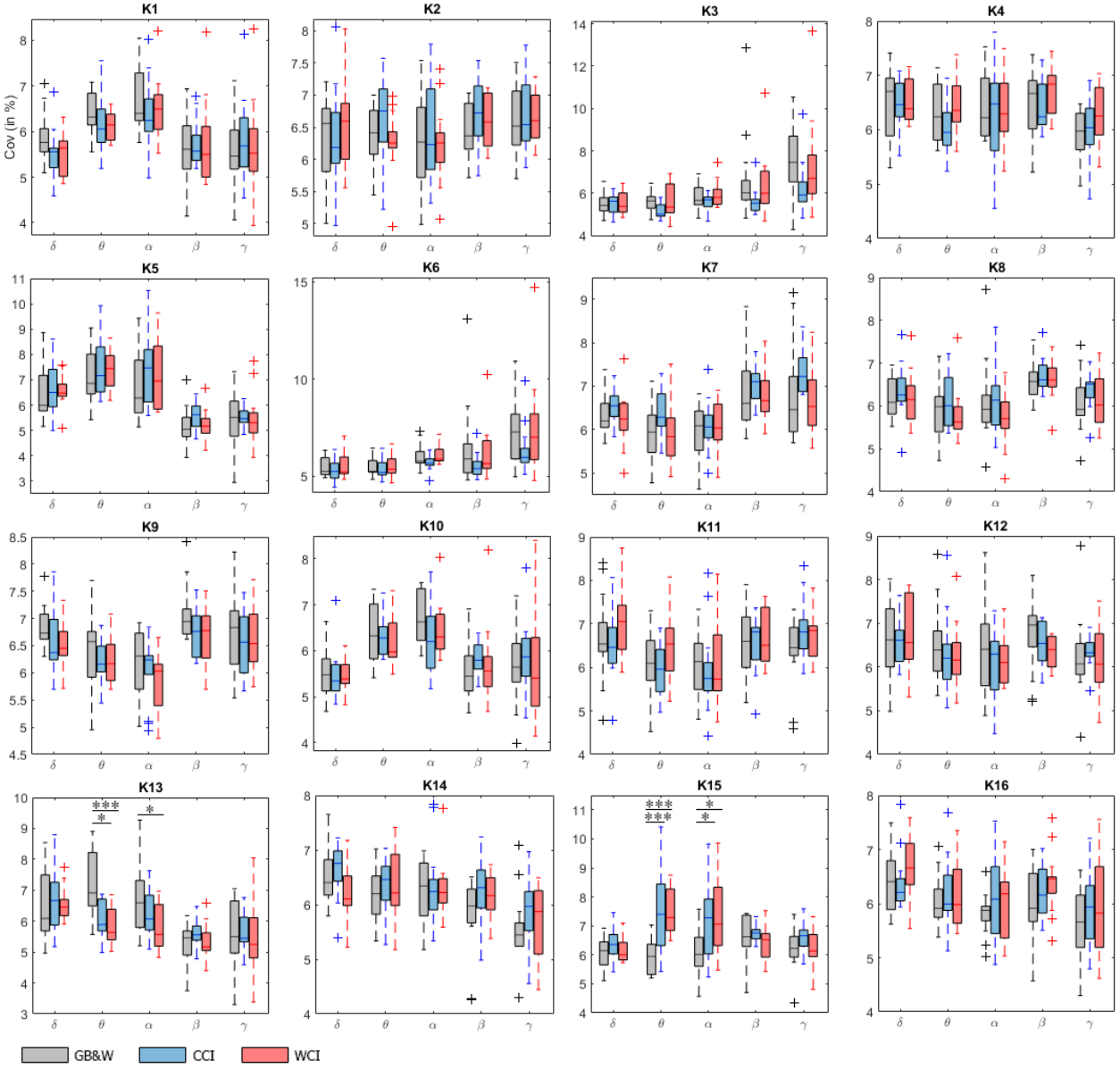

FIGURE 5. Boxplots show coverage (in %) of each cluster for all three groups (GB&W, CCI, WCI) and for five frequency bands (δ, θ, α, β, γ). Asterisks indicate the significance level ($*p < 0.05$ and $***p < 0.0005$).

The STP matrices, averaged over participants, were determined for each condition, and the results are presented in Supplementary Figs. S4-S6. In the δ band, high probability values along the diagonal indicate the likelihood of remaining in the same state (i.e., self-transitions). These results are consistent with the temporal trends in mean duration (significantly longer duration at a particular state in the δ band than in the other four frequency bands (θ, α, β, and γ), where MD is in the range of 225–235 ms) are displayed in Supplementary Figs. S1-S3. In the θ band, the STP also seems to have high values along the diagonal, albeit at a lower probability, and the MD is shorter than that of the δ band. Only a few STP elements showed high probabilities in the α, β and γ bands. On average, the four frequency bands (θ, α, β and γ) had an MD in the range of 200–210 ms.

B. RECURRING PATTERNS OF DIRECTED CONNECTIVITY NETWORKS ACROSS FREQUENCIES AND CONDITIONS

The previous subsection presented the results of the recurrences of directed connectivity networks across frequency bands in the individual condition. This section presents the results of directed connectivity networks shared among all conditions, which enables us to determine the differences in coverage, mean duration, and state transition probability of the color effect on directed connectivity networks between frequency bands across groups. Fig. 4 shows the repeated patterns of directed connectivity networks, which are shared among all conditions.

One-way MANOVA showed that there were statistically significant differences in cluster coverage based on the

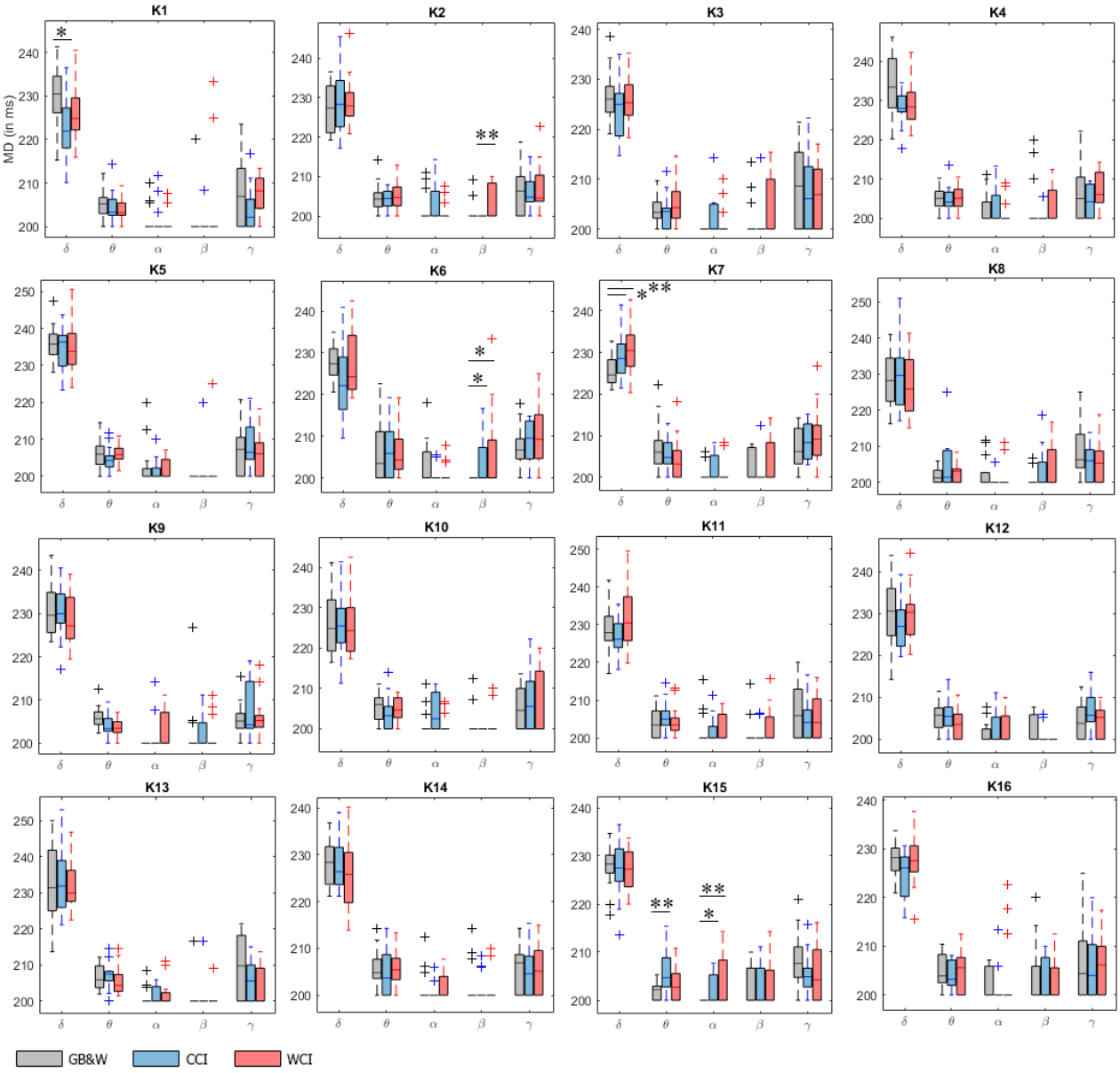

FIGURE 6. Boxplots show mean duration (in ms) of each cluster for all three groups (GB&W, CCI, WCI) and for five frequency bands (δ, θ, α, β, γ). Asterisks indicate the significance level ($*p < 0.05$ and $**p < 0.005$).

participants' learning conditions: K13 ($F(10, 70) = 2.62$, $p < 0.05$; Wilk's $\Lambda = 0.529$, partial $\eta^2 = 0.27$) and K15 ($F(10, 70) = 2.62$, $p < 0.05$; Wilk's $\Lambda = 0.529$, partial $\eta^2 = 0.27$). Specifically, significant effects on θ ($F(2, 39) = 11.09$, $p < 0.0005$, partial $\eta^2 = 0.36$) and α bands ($F(2, 39) = 3.89$, $p < 0.05$, partial $\eta^2 = 0.17$) at K13. Post-hoc tests revealed that the mean coverage for K13 in θ band showed a significant difference between GB&W and CCI ($p < 0.05$) and GB&W and WCI ($p < 0.0005$), but not between CCI and WCI ($p = 0.390$). The mean coverage for K13 in α band showed a significant difference between GB&W and WCI ($p < 0.05$), but not between GB&W and CCI ($p = 0.138$) or CCI and WCI ($p = 0.211$).

A similar pattern of coverage differences between frequency bands was observed for K15, with a significant effect found at θ ($F(2, 39) = 11.11$, $p < 0.0005$, partial $\eta^2 = 0.37$) and α bands ($F(2, 39) = 6.80$, $p < 0.05$, partial $\eta^2 = 0.20$). In the θ band, the mean coverage for K15 showed a significant difference between GB&W and CCI ($p < 0.0005$) and GB&W and WCI ($p < 0.0005$) but not between CCI and WCI ($p = 0.955$). In the α band, the same trends of significant differences were found between GB&W and CCI ($p < 0.05$) and GB&W and WCI ($p < 0.05$), but not between CCI and WCI ($p = 0.710$).

MD was also computed for each estimated directed connectivity network. From the results of the Kruskal-Wallis

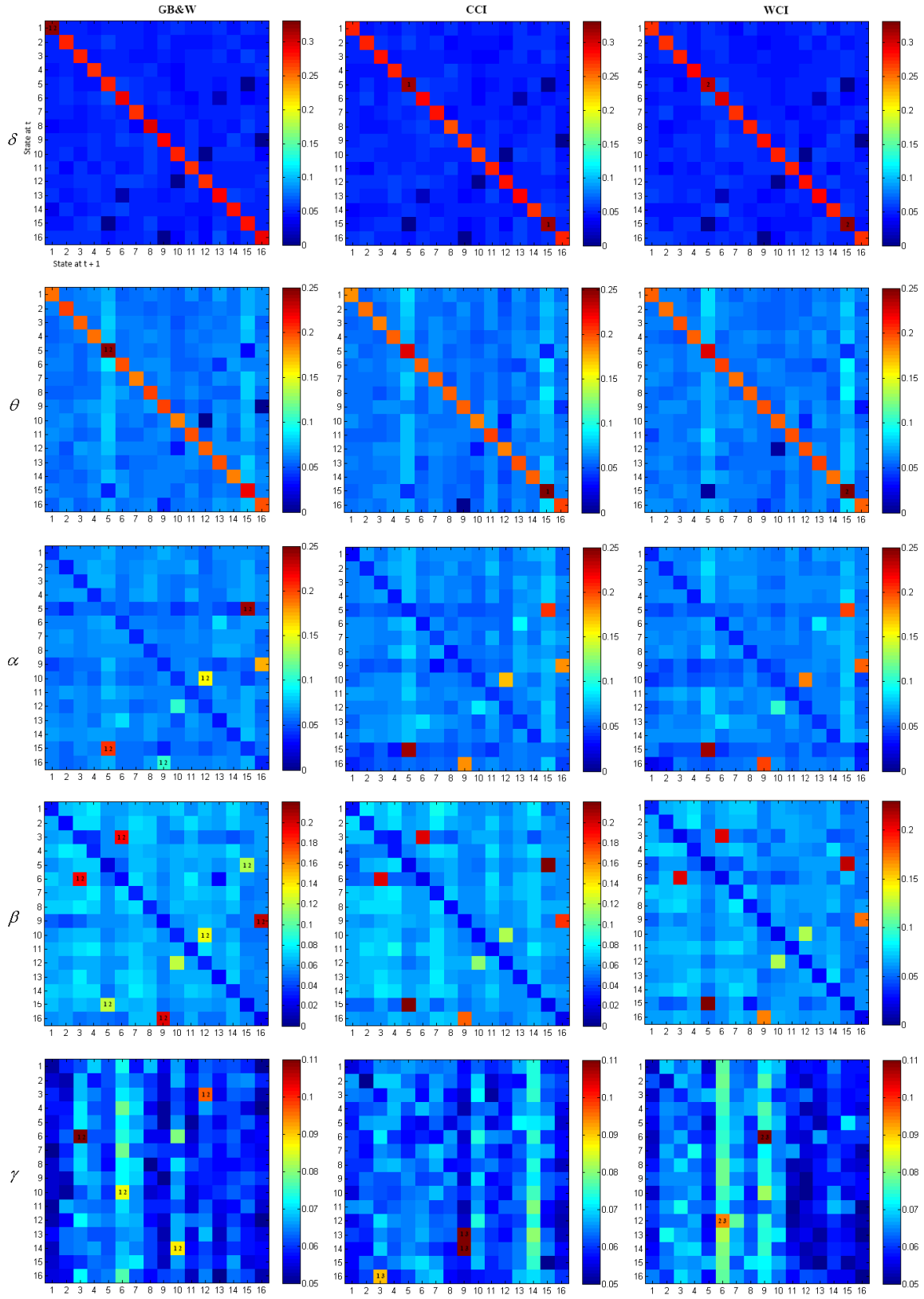

FIGURE 7. Between-group analysis: The state transition probability (STP) matrix, averaged over subjects (left: GB&W, middle: CCI, right: WCI) for five EEG bands, δ, θ, α, β, γ, respectively. Numbers indicate the differences between frequency bands at the significance level ($p < 0.005$, Bonferroni-corrected). Number 1: GB&W vs. CCI, Number 2: GB&W vs. WCI, Number 3: CCI vs. WCI. Red colors indicate a high probability for switching between the two states; Blue colors indicate a low probability for switching between the two states.

H test for MD, there were significant differences observed in four frequency bands (δ, θ, α and β) between the three experimental conditions:1) K1 ($\chi^2(2) = 6.826$, $p = 0.033$) and K7 ($\chi^2(2) = 8.043$, $p = 0.018$) in the δ band; 2) K15 ($\chi^2(2) = 7.865$, $p = 0.020$) in the θ band; 3) K15 ($\chi^2(2) = 7.686$, $p = 0.021$) in the α band; and 4) K2 ($\chi^2(2) = 8.498$, $p = 0.014$) and K6 ($\chi^2(2) = 6.274$, $p = 0.043$) in the β band. Post-hoc tests revealed that there was a statistically significant difference in MD between the GB&W and CCI conditions ($U = 46.5$, $p = 0.018$) in the δ band, indicating that the GB&W condition stayed for a longer time at K1, as compared to the CCI condition. Moreover, the CCI ($U = 52.0$, $p = 0.035$) and WCI ($U = 40.0$, $p = 0.008$) conditions remained longer at K7 than at the GB&W condition. For θ band, the CCI condition required a longer time at K15 ($U = 38.5$, $p = 0.006$) than the GB&W condition. In the α band, the CCI and WCI conditions required a longer time at K15 ($U = 70$, $p = 0.034$ and $U = 56$, $p = 0.007$, respectively) than the GB&W condition. Lastly, in the β band, the WCI condition spent a longer time at K2 ($U = 56.0$, $p = 0.007$) than the CCI condition. Moreover, CCI ($U = 63.0$, $p = 0.016$) and WCI ($U = 63.0$, $p = 0.016$) conditions stayed longer at K6 than at the GB&W condition. Figs. 5 and 6 show boxplots summarizing the results for the coverage and mean duration, respectively.

Finally, the mean STP matrices results for each condition and frequency band are presented in Fig. 7. As shown in Fig. 7, high probability values along the diagonal indicate the likelihood of remaining in the same state before it switches to another state (self-transitions) in the lower frequency bands (δ and θ bands), regardless of the experimental conditions. These results are consistent with the temporal trends in the mean duration (i.e., stayed longer at a particular state in the lower frequency bands) displayed in Fig. 6. However, there was a significant difference in the STP between the experimental conditions. In particular, in the δ band, there was a preference for self-transition of K1 (K1→K1) in GB&W compared to the CCI and WCI conditions; in contrast, there was a preference for self-transition of K5 (K5→K5) and K15 (K15→K15) in both CCI and WCI conditions compared to GB&W. In the θ band, there was a preference for self-transition of K5 in GB&W compared to the CCI and WCI conditions, whereas there was a preference for self-transition of K15 (K15→K15) in both the CCI and WCI conditions compared to GB&W. In addition, there is a significant reversal in the state transition pattern. The state transition from K15 to K5 (K15→K5) was found in the CCI and WCI conditions compared to the GB&W condition (an inverse state transition, K5→K15) in the α band, indicating that brain states are important in perceiving incoming information and behavioral responses in maintaining performance.

IV. DISCUSSION

This study assessed the temporal variability and repeatability of directed connectivity networks over time and frequency domains, which is because interactions among different brain regions are inherently dynamic. The experimental results showed that patterns of the brain dynamic directed connectivity networks formed a set of quasi-stable states that recurred over time and frequency, suggesting that the directed connectivity network in the brain is indeed dynamic and dependent on specific EEG frequency bands that may exist at multiple frequency bands. First, we observed that certain brain states are more dominant than others at particular frequency bands, and the dominant states were shared by more than one frequency band that was mostly found between θ and α bands or between β and γ bands. Second, microstate analysis showed that the mean duration of brain states was longer in the lower frequency bands (δ and θ bands) than in the higher frequency bands (α, β and γ bands), indicating that the mean duration of the microstate is dependent on specific frequency bands. The lower frequency bands (i.e., δ, θ) have a higher probability of self-transitions than the higher frequency bands. Overall, the colored multimedia learning materials affects the information flow in the brain during learning, as is reflected by the features of the microstate (coverage, mean duration, and state transition probability) of directed connectivity networks in the five EEG frequency bands associated with emotion and cognitive processes (attention, perception, working memory, and memory) involved in human learning. Top-down and bottom-up interactions influence the allocation of attention and perception towards learning materials. Color also appears to have a modulatory effect on the processing of visuospatial information in working memory, which prioritizes sensory input and manipulates information selection during learning, facilitating memory processing (encoding and retention).

Table 1 shows that some of the brain states were shared between low-frequency bands (θ and α bands) and high-frequency bands (β and γ bands), demonstrating that the coverage of the directed connectivity network is dependent on the specific frequency bands and may exist in more than one frequency band. These results confirmed that neurons oscillating at different frequency bands might contribute to the same functional network, which is consistent with the findings of an EEG-fMRI study [55]. In addition, increased coverage of long-range connectivity (frontal and posterior regions) occurs in the θ and α bands, which are associated with attentional and memory processes, whereas short-range connectivity in the higher frequency bands (β and γ) is related to sensory processing [56], suggesting a relationship between directed connectivity networks and EEG frequency bands. This finding is consistent with earlier studies; long-range and short-range connectivity is mediated by lower and higher frequency bands, respectively [57], [58], [59].

Moreover, correlation analysis revealed that some brain states were highly correlated between conditions, whereas others were specific (unique) to a particular condition. These findings highlight the need for (1) individual analysis of each condition to identify dynamic changes in directed connectivity patterns that recur in time and frequency domains,

and (2) a joint analysis of all conditions to identify the potential psychophysiological indicator/biomarker to assess the changes in emotional/cognitive responses to colored vs. achromatic learning materials, using temporal parameters (coverage, mean duration, STP, etc.) [33], [35].

The results obtained from the cluster analysis and dynamic state computation showed that each brain microstate might remain stable for a particular period of time (∼hundreds of milliseconds) and then shift to another microstate and remain stable again. This is consistent with previous microstate studies [34], [60]. It is observed that the mean duration of all microstates in the δ band compared to the other four EEG bands (θ, α, β, γ) in all three groups potentially reflects δ band as the slow wave of the EEG signal. They are more likely to remain in the same state for consecutive time points (self-transitions). Our data also demonstrate that the mean duration of certain microstates differs in certain frequency bands under respective conditions: (i) two microstates (K3 and K9) had significantly lengthened mean duration in the θ band compared to α and β bands, and two microstates (K6 and K15) significantly lengthened the mean duration in the θ band compared to the α band in the GB&W group; (ii) two microstates (k9 and K13) significantly increased in duration in the θ band compared to the α band and β band, respectively, in the CCI group; (iii) a significant increase in the duration of the three microstates (K5, K12, and K14) in the θ band compared to the α band, and one microstate (K12) had a longer duration in the α band than γ band in the WCI group. The overall mean duration of the microstates was longer in the lower frequency bands (δ and θ bands) than in the higher frequency bands (α, β and γ bands), indicating that the microstate's mean duration is dependent on specific frequency bands.

The lower frequency bands (i.e., δ, θ) have a higher probability of self-transitions, indicating that these bands are more likely to stay in the same state before they switch to another state. However, only a few state transitions show high probabilities in the α, β, and γ bands, which differ between the conditions. These results indicate that dynamic switching between different brain states is a manifestation of certain directed brain states that play a dominant role during the processing of visuospatial information in working memory and attention, prioritizing sensory input during learning in the presence of color. In addition, the mean duration of the microstates was longer in the lower frequency bands (δ and θ bands) than in the higher frequency bands (α, β and γ bands). These findings indicate that the dynamic directed connectivity networks derived from EEG signals are frequency dependent. The change in the temporal properties of dynamic directed connectivity networks can be a constitutive EEG parameter for assessing visual color influences on brain information processing during a learning task. This is in agreement with the results reported by other researchers that mental activity or information processing occurs through a sequence of quasi-stable states [61], and that an increase in the mean duration of certain microstates is related to cognitive tasks [62] and information processing that gives rise to our conscious experience [34]. Thus, future studies may consider narrow-band (i.e., frequency-specific) EEG microstates of dynamic directed connectivity network analysis to identify meaningful network dynamics related to cognition, perception, or behavioral variability that include participants of different ages. In addition, the temporal dynamics of directed connectivity networks can be combined with other EEG features to improve the classification accuracy of cognitive states. A recent study [63] showed that the fusion of EEG local activation parameters and brain connectivity patterns provides a better classification performance in detecting cognitive states compared to a single EEG feature.

In addition, the results of the between-group analysis (Section III-B) further showed that the predominant state (increased mean coverage of K15) was formed between the anterior areas (prefrontal and frontal cortices) and posterior regions (temporal, parietal, and occipital cortices), where the direction of information flows from anterior to posterior brain regions during learning (for both CCI and WCI conditions). Similarly, the mean duration of K15 increased significantly in the CCI and WCI conditions compared with GB&W in the θ and α bands. The trend of increasing coverage and mean duration of K15 during the learning task when participants viewed colored materials compared to achromatic materials indicated stronger interactions between the central executive network areas and higher-order association areas stimulated by color. The prefrontal cortex region seems to exert top-down attentional control while manipulating information selection in the working memory for encoding, which might contribute to efficient information processing. This could be due to the dominant role of the prefrontal and frontal cortices during the processing of visuospatial information in working memory and selecting the sensory input during learning, which facilitates successful learning in the presence of color [64]. These data-driven results agree with previous studies performed by other researchers. Earlier EEG studies have reported that θ and α bands play an important role in attention, memory processes, alertness state, and emotional and motivational processes [46], [65], [66], [67], which eventually facilitate faster and more accurate memory performance. Therefore, the temporal dynamics of frequency-specific directed connectivity networks may open the way to various investigations of cognitive and emotional processes.

The findings of this study are consistent with those of previous reports [32], [64]. They are indirectly associated with top-down attentional processes in θ and α bands due to emotional responses to color in the dorsolateral prefrontal cortex (DLPFC) and ventrolateral prefrontal cortex (VLPFC), which are associated with working memory and emotional regulation processes [16]. Recent electrophysiological and fMRI results provide evidence of top-down attentional modulation in the frontal cortex, which reveals preferential

engagement with external attention [68], and the brain processes color information in a directional manner. The neural representation instantiated by color drives semantic/cognitive representation [69], and the pattern of neural activity elicited by color is reactivated later, revealing the temporal dynamics of color processing [70]. Moreover, color has been found to evoke emotional experiences and modulate global connectivity [71]. This is consistent with our previous study [12] on the direction of information flow from the anterior to posterior brain regions during learning (CCI and WCI conditions) in the θ and α bands.

In addition, the present study indicates that both CCI and WCI conditions stayed for a longer time and increased coverage at state K15 in the θ and α bands compared to the GB&W condition. The mean STP also shows a different state transition pattern between K5 and K15. The state transition from K15 to K5 was found in the CCI and WCI conditions compared to the GB&W condition (an inverse state transition from K5 to K15) in the α band, indicating that the brain states were important for perceiving incoming information, emotional, behavioral, and adaptive responses in maintaining performance. This suggests that color might have stimulated top-down modulation of working memory, that is, enhancing anticipatory control over encoding and retention [14] and selective attention, which in turn improves learning [72]. We also believe that the prefrontal and frontal cortices are important in driving positive emotional experiences, maintaining motivation, and influencing learning and memory performance. Enhanced selective attention and positive emotional states facilitate the integration of sensory and perceptual information stored in different brain areas via a bottom-up approach to higher brain functions. This could be possibly due to increased behavioral intention and anticipation in the colored conditions compared to the GB&W condition. A recent EEG study [73] showed that a lecture video with a color-coded design elicited positive emotions that were associated with lower cognitive load. Hence, instructors can use warm/cold colors rather than achromatic colors to provide positive emotional experiences throughout the learning process and to enhance cognitive functions.

The overall results showed that directed connectivity in the brain during learning is indeed dynamic; that is, not only is one brain area active at a given moment, but many regions are active and form distinct patterns of synchronized activity (brain states) that vary over time and are dependent on frequency bands, which is in agreement with the results reported by other researchers [36], [74]. It further investigates the integration of emotional and cognitive information processing and how brain data can support behavioral responses and adaptive processes [64], [67], [75]. The present work extends previous studies by illustrating how a dynamic directed connectivity network with microstate analysis can reveal more insightful information about the recurring patterns of directed interactions among different brain regions in a data-driven manner. We provide further evidence that the temporal parameters of directed connectivity networks differ in specific frequency bands with respect to color conditions, demonstrating that visual color affects brain information processing, which is not quantifiable through static brain connectivity analysis. Perhaps it could be implemented for classroom/virtual learning to monitor learners' mental states during learning (attention, concentration, alertness, emotion, motivation, boredom, etc.) to keep learners focused while studying and completing the ongoing tasks by providing optimum sensory stimulation through visuals or sounds (interactive quizzes, attractive and informative illustrations, music, etc.). As color has an exceptional ability to capture visual attention and enhance positive emotions [2], [3], [4], it is especially useful in educational settings to draw students' attention and stimulate them to read, learn, acquire, and retain knowledge. In addition, studies have found that listening to sounds of nature [76], [77] can reduce stress and elicit pleasure and relaxation, which improve various aspects of cognition and emotion. In combination, these can promote effective learning and long-term memory retention.

V. LIMITATIONS AND FUTURE WORK

K-means clustering is a clustering algorithm capable of grouping similar brain networks to identify recurring patterns of directed networks. It is also a data-driven approach that allows the examination of data, even with limited or no a priori information. However, a disadvantage of this clustering algorithm is the number of clusters necessary for capturing useful features from the data. A similar issue was encountered when employing the independent component analysis [60]. In this study, we searched for a range between 2 and 20 clusters and used the explained variance method to determine the optimal number of clusters. Future work will explore other clustering techniques, such as hierarchical, density-based, and model-based clustering, which do not require pre-specifying the number of clusters.

CSD transformation can be used for brain connectivity estimation in sensor space [11], [78], [79] to reduce spurious connections. However, it is recommended that brain connectivity estimation should be performed on the source signals from high-density EEG recordings along with simultaneous fMRI scanning and then estimated using appropriate connectivity measures (insensitive to volume conduction effect) [80], [81] to obtain a better estimation of the functional, directed, or effective connectivity and provide a more accurate interpretation of the underlying connectivity dynamics (active interactions between brain sources) [82], [83]. It is also important to compare the results of the whole pipeline of source reconstruction and connectivity estimation by using different combinations of forward and inverse models and connectivity measures owing to the limitations of 1) source reconstruction caused by residual signal leakage at the source level and 2) estimation of connectivity caused by source mixing. Therefore, our next step is to compare the results of different forward and inverse models to overcome the limitations of the present study.

Finally, in terms of computational complexity, the proposed method is based on a traditional model-free, nonparametric approach; thus, it has a lower model complexity and computational cost. Compared with static brain connectivity analysis, additional computational time is required to assess the statistical testing of dynamic data points. To implement real-time processing, dimensionality reduction may be required to reduce redundancy and computational demands if larger data are involved.

VI. CONCLUSION

This study investigated the effects of color visuals on information processing by brain during learning using a new analytical method, wavelet-based PSI, based on a combination of wavelet transform and phase slope index for dynamic directed connectivity network analysis. The temporal parameters of the directed connectivity networks in the time and frequency domains were determined using a microstate analysis. The experimental results revealed that the reoccurrence of a brain state, its coverage, and the amount of time the brain remained in a particular state varied. Our analysis revealed common brain states that are repeatedly present in different frequency bands, and identified that certain states are unique to specific conditions (participants viewed multimedia learning materials with visual illustrations displayed in achromatic, cool, or warm colors). The processing of information differs owing to the influence of visual colors. The allocation of attention and perception towards learning materials was influenced by top-down and bottom-up interactions; thus, the our study results provide quantitative evidence of the estimation of the dynamic directed connectivity networks, which can provide an objective assessment of the learning process with emotional design materials to create a better understanding of the process of learning and how this information can be used to create more effective multimedia learning materials and environments. Such microstates of dynamic directed connectivity networks could serve as psychophysiological indicators (characteristic of learning) to help understand how neuronal synchronization during the learning process is owing to the changes in cognitive, emotional, and attentional states that govern our behavior. Thus, further investigations should consider the dynamic analysis not only of the connectivity network changes in frequency bands, but also the network patterns that repeat over time to provide a deeper understanding of the learning and memory processes.

REFERENCES

[1] S. Erk, M. Kiefer, J. O. Grothe, A. P. Wunderlich, M. Spitzer, and H. Walter, "Emotional context modulates subsequent memory effect," *NeuroImage*, vol. 18, no. 2, pp. 439–447, Feb. 2003.

[2] J. L. Plass, S. Heidig, E. O. Hayward, B. D. Homer, and E. Um, "Emotional design in multimedia learning: Effects of shape and color on affect and learning," *Learn. Instruct.*, vol. 29, pp. 128–140, Feb. 2014.

[3] E. Um, J. L. Plass, E. O. Hayward, and B. D. Homer, "Emotional design in multimedia learning," *J. Educ. Psychol.*, vol. 104, pp. 485–499, May 2012.

[4] R. E. Mayer and G. Estrella, "Benefits of emotional design in multimedia instruction," *Learn. Instruct.*, vol. 33, pp. 12–18, Oct. 2014.

[5] B. Park, L. Knörzer, J. L. Plass, and R. Brünken, "Emotional design and positive emotions in multimedia learning: An eyetracking study on the use of anthropomorphisms," *Comput. Educ.*, vol. 86, pp. 30–42, Aug. 2015.

[6] C. Brom, T. Stárková, J. Lukavský, O. Javora, and E. Bromová, "Eye tracking in emotional design research: What are its limitations?" in *Proc. 9th Nordic Conf. Hum.-Comput. Interact.*, Oct. 2016, p. 114.

[7] X. Wang, R. E. Mayer, M. Han, and L. Zhang, "Two emotional design features are more effective than one in multimedia learning," *J. Educ. Comput. Res.*, vol. 60, no. 8, pp. 1991–2014, Jan. 2023.

[8] A. M. Uzun and Z. Yıldırım, "Exploring the effect of using different levels of emotional design features in multimedia science learning," *Comput. Educ.*, vol. 119, pp. 112–128, Apr. 2018.

[9] Y. Le, J. Liu, C. Deng, and D. Y. Dai, "Heart rate variability reflects the effects of emotional design principle on mental effort in multimedia learning," *Comput. Hum. Behav.*, vol. 89, pp. 40–47, Dec. 2018.

[10] R. Abreu, A. Leal, and P. Figueiredo, "EEG-informed fMRI: A review of data analysis methods," *Frontiers Hum. Neurosci.*, vol. 12, p. 29, Feb. 2018.

[11] X. Li, B. Mota, T. Kondo, S. Nasuto, and Y. Hayashi, "EEG dynamical network analysis method reveals the neural signature of visual-motor coordination," *PLoS ONE*, vol. 15, no. 5, May 2020, Art. no. e0231767.

[12] M. T. Chai, H. U. Amin, L. I. Izhar, M. N. M. Saad, M. Abdul Rahman, A. S. Malik, and T. B. Tang, "Exploring EEG effective connectivity network in estimating influence of color on emotion and memory," *Frontiers Neuroinform.*, vol. 13, p. 66, Oct. 2019.

[13] M. Rubinov and O. Sporns, "Complex network measures of brain connectivity: Uses and interpretations," *NeuroImage*, vol. 52, no. 3, pp. 1059–1069, Sep. 2010.

[14] T. P. Zanto, M. T. Rubens, J. Bollinger, and A. Gazzaley, "Top-down modulation of visual feature processing: The role of the inferior frontal junction," *NeuroImage*, vol. 53, no. 2, pp. 736–745, Nov. 2010.

[15] P. Vuilleumier, "How brains beware: Neural mechanisms of emotional attention," *Trends Cognit. Sci.*, vol. 9, no. 12, pp. 585–594, Dec. 2005.

[16] J. T. Buhle, J. A. Silvers, T. D. Wager, R. Lopez, C. Onyemekwu, H. Kober, J. Weber, and K. N. Ochsner, "Cognitive reappraisal of emotion: A meta-analysis of human neuroimaging studies," *Cerebral Cortex*, vol. 24, no. 11, pp. 2981–2990, Nov. 2014.

[17] A. Razi and K. J. Friston, "The connected brain: Causality, models, and intrinsic dynamics," *IEEE Signal Process. Mag.*, vol. 33, no. 3, pp. 14–35, May 2016.

[18] A. T. Reid, D. B. Headley, R. D. Mill, R. Sanchez-Romero, L. Q. Uddin, D. Marinazzo, D. J. Lurie, P. A. Valdés-Sosa, S. J. Hanson, B. B. Biswal, V. Calhoun, R. A. Poldrack, and M. W. Cole, "Advancing functional connectivity research from association to causation," *Nature Neurosci.*, vol. 22, no. 11, pp. 1751–1760, Nov. 2019.

[19] M. Arnold, X. H. R. Milner, H. Witte, R. Bauer, and C. Braun, "Adaptive AR modeling of nonstationary time series by means of Kalman filtering," *IEEE Trans. Biomed. Eng.*, vol. 45, no. 5, pp. 553–562, May 1998.

[20] W. Hesse, E. Möller, M. Arnold, and B. Schack, "The use of time-variant EEG Granger causality for inspecting directed interdependencies of neural assemblies," *J. Neurosci. Methods*, vol. 124, no. 1, pp. 27–44, Mar. 2003.

[21] B. Schack, "Dynamic topographic spectral analysis of cognitive processes," in *Analysis of Neurophysiological Brain Functioning*. Cham, Switzerland: Springer, 1999, pp. 230–251.

[22] T. Milde, L. Leistritz, L. Astolfi, W. H. R. Miltner, T. Weiss, F. Babiloni, and H. Witte, "A new Kalman filter approach for the estimation of high-dimensional time-variant multivariate AR models and its application in analysis of laser-evoked brain potentials," *NeuroImage*, vol. 50, no. 3, pp. 960–969, Apr. 2010.

[23] E. G. Ghumare, M. Schrooten, R. Vandenberghe, and P. Dupont, "A time-varying connectivity analysis from distributed EEG sources: A simulation study," *Brain Topography*, vol. 31, no. 5, pp. 721–737, Sep. 2018.

[24] M. G. Preti, T. A. W. Bolton, and D. Van De Ville, "The dynamic functional connectome: State-of-the-art and perspectives," *Neuroimage*, vol. 160, pp. 41–54, Oct. 2017.

[25] G. C. O'Neill, P. Tewarie, D. Vidaurre, L. Liuzzi, M. W. Woolrich, and M. J. Brookes, "Dynamics of large-scale electrophysiological networks: A technical review," *NeuroImage*, vol. 180, pp. 559–576, Oct. 2018.

[26] M. Kaminski and H. Liang, "Causal influence: Advances in neurosignal analysis," *Critical Rev. Biomed. Eng.*, vol. 33, no. 4, pp. 347–430, 2005.

[27] V. D. Calhoun and T. Adali, "Time-varying brain connectivity in fMRI data: Whole-brain data-driven approaches for capturing and characterizing dynamic states," *IEEE Signal Process. Mag.*, vol. 33, no. 3, pp. 52–66, May 2016.

[28] M. F. Pagnotta, M. Dhamala, and G. Plomp, "Benchmarking nonparametric Granger causality: Robustness against downsampling and influence of spectral decomposition parameters," *NeuroImage*, vol. 183, pp. 478–494, Dec. 2018.

[29] M. Dhamala, "Analyzing information flow in brain networks with nonparametric Granger causality," *NeuroImage*, vol. 41, pp. 354–362, Jun. 2008.

[30] H. Adeli, Z. Zhou, and N. Dadmehr, "Analysis of EEG records in an epileptic patient using wavelet transform," *J. Neurosci. Methods*, vol. 123, no. 1, pp. 69–87, Feb. 2003.

[31] S. I. Dimitriadis, N. A. Laskaris, V. Tsirka, M. Vourkas, S. Micheloyannis, and S. Fotopoulos, "Tracking brain dynamics via time-dependent network analysis," *J. Neurosci. Methods*, vol. 193, no. 1, pp. 145–155, Oct. 2010.

[32] T. P. Zanto, M. T. Rubens, A. Thangavel, and A. Gazzaley, "Causal role of the prefrontal cortex in top-down modulation of visual processing and working memory," *Nature Neurosci.*, vol. 14, no. 5, pp. 656–661, 2011.

[33] M. Yaesoubi, E. A. Allen, R. L. Miller, and V. D. Calhoun, "Dynamic coherence analysis of resting fMRI data to jointly capture state-based phase, frequency, and time-domain information," *NeuroImage*, vol. 120, pp. 133–142, Oct. 2015.

[34] D. Lehmann, H. Ozaki, and I. Pal, "EEG alpha map series: Brain microstates by space-oriented adaptive segmentation," *Electroencephalogr. Clin. Neurophysiol.*, vol. 67, no. 3, pp. 271–288, Sep. 1987.

[35] C. M. Michel and T. Koenig, "EEG microstates as a tool for studying the temporal dynamics of whole-brain neuronal networks: A review," *NeuroImage*, vol. 180, pp. 577–593, Oct. 2018.

[36] M. Bola and B. A. Sabel, "Dynamic reorganization of brain functional networks during cognition," *Neuroimage*, vol. 114, pp. 398–413, Jul. 2015.

[37] C. Zhang, L. Sun, F. Cong, and T. Ristaniemi, "Spatiotemporal dynamical analysis of brain activity during mental fatigue process," *IEEE Trans. Cognit. Develop. Syst.*, vol. 13, no. 3, pp. 593–606, Sep. 2021.

[38] E. A. Allen, E. Damaraju, S. M. Plis, E. B. Erhardt, T. Eichele, and V. D. Calhoun, "Tracking whole-brain connectivity dynamics in the resting state," *Cerebral Cortex*, vol. 24, no. 3, pp. 663–676, 2014.

[39] A. Kabbara, W. E. Falou, M. Khalil, F. Wendling, and M. Hassan, "The dynamic functional core network of the human brain at rest," *Sci. Rep.*, vol. 7, no. 1, p. 2936, Jun. 2017.

[40] G. Nolte, A. Ziehe, V. V. Nikulin, A. Schlögl, N. Krämer, T. Brismar, and K.-R. Müller, "Robustly estimating the flow direction of information in complex physical systems," *Phys. Rev. Lett.*, vol. 100, no. 23, pp. 234101–234104, Jun. 2008.

[41] J. A. Urigüen and B. Garcia-Zapirain, "EEG artifact removal—State-of-the-art and guidelines," *J. Neural Eng.*, vol. 12, Apr. 2015, Art. no. 031001.

[42] J. Kayser and C. E. Tenke, "Principal components analysis of Laplacian waveforms as a generic method for identifying ERP generator patterns: II. Adequacy of low-density estimates," *Clin. Neurophysiol.*, vol. 117, no. 2, pp. 369–380, Feb. 2006.

[43] F. Perrin, J. Pernier, O. Bertrand, and J. F. Echallier, "Spherical splines for scalp potential and current density mapping," *Electroencephalogr. Clin. Neurophysiol.*, vol. 72, no. 2, pp. 184–187, Feb. 1989.

[44] A. Delorme and S. Makeig, "EEGLAB: An open source toolbox for analysis of single-trial EEG dynamics including independent component analysis," *J. Neurosci. Methods*, vol. 134, no. 1, pp. 9–21, Mar. 2004.

[45] M. X. Cohen, *Analyzing Neural Time Series Data: Theory and Practice*. Cambridge, MA: MIT Press, 2014.

[46] W. Klimesch, "Alpha-band oscillations, attention, and controlled access to stored information," *Trends Cogn. Sci.*, vol. 16, no. 12, pp. 606–617, Dec. 2012.

[47] X.-J. Wang, "Neurophysiological and computational principles of cortical rhythms in cognition," *Physiolog. Rev.*, vol. 90, no. 3, pp. 1195–1268, Jul. 2010.

[48] M. Dipoppa and B. S. Gutkin, "Flexible frequency control of cortical oscillations enables computations required for working memory," *Proc. Nat. Acad. Sci. USA*, vol. 110, no. 31, pp. 12828–12833, Jul. 2013.

[49] G. Nolte, O. Bai, L. Wheaton, Z. Mari, S. Vorbach, and M. Hallett, "Identifying true brain interaction from EEG data using the imaginary part of coherency," *Clin. Neurophysiol.*, vol. 115, pp. 2292–2307, Oct. 2004.

[50] E. Bullmore and O. Sporns, "Complex brain networks: Graph theoretical analysis of structural and functional systems," *Nature Rev. Neurosci.*, vol. 10, no. 3, pp. 186–198, Mar. 2009.

[51] E. Maris and R. Oostenveld, "Nonparametric statistical testing of EEG- and MEG-data," *J. Neurosci. Methods*, vol. 164, no. 1, pp. 177–190, Aug. 2007.

[52] S. Lloyd, "Least squares quantization in PCM," *IEEE Trans. Inf. Theory*, vol. IT-28, no. 2, pp. 129–137, Mar. 1982.

[53] J. van Driel, E. Gunseli, M. Meeter, and C. N. L. Olivers, "Local and interregional alpha EEG dynamics dissociate between memory for search and memory for recognition," *NeuroImage*, vol. 149, pp. 114–128, Apr. 2017.

[54] J. Zheng, K. L. Anderson, S. L. Leal, A. Shestyuk, G. Gulsen, L. Mnatsakanyan, S. Vadera, F. P. K. Hsu, M. A. Yassa, R. T. Knight, and J. J. Lin, "Amygdala-hippocampal dynamics during salient information processing," *Nature Commun.*, vol. 8, no. 1, Feb. 2017, Art. no. 14413.

[55] D. Mantini, M. G. Perrucci, C. Del Gratta, G. L. Romani, and M. Corbetta, "Electrophysiological signatures of resting state networks in the human brain," *Proc. Nat. Acad. Sci. USA*, vol. 104, no. 32, pp. 13170–13175, Aug. 2007.

[56] K. Jann, M. Kottlow, T. Dierks, C. Boesch, and T. Koenig, "Topographic electrophysiological signatures of fMRI resting state networks," *PLoS ONE*, vol. 5, no. 9, Sep. 2010, Art. no. e12945.

[57] M. Ganzetti and D. Mantini, "Functional connectivity and oscillatory neuronal activity in the resting human brain," *Neuroscience*, vol. 240, pp. 297–309, Jun. 2013.

[58] N. Kopell, G. Ermentrout, M. Whittington, and R. Traub, "Gamma rhythms and beta rhythms have different synchronization properties," *Proc. Nat. Acad. Sci. USA*, vol. 97, pp. 1867–1872, Feb. 2000.

[59] J. Samogin, Q. Liu, M. Marino, N. Wenderoth, and D. Mantini, "Shared and connection-specific intrinsic interactions in the default mode network," *NeuroImage*, vol. 200, pp. 474–481, Oct. 2019.

[60] R. D. Pascual-Marqui, C. M. Michel, and D. Lehmann, "Segmentation of brain electrical activity into microstates: Model estimation and validation," *IEEE Trans. Biomed. Eng.*, vol. 42, no. 7, pp. 658–665, Jul. 1995.

[61] A. A. Fingelkurts and A. A. Fingelkurts, "Timing in cognition and EEG brain dynamics: Discreteness versus continuity," *Cognit. Process.*, vol. 7, no. 3, pp. 135–162, Sep. 2006.

[62] B. A. Seitzman, M. Abell, S. C. Bartley, M. A. Erickson, A. R. Bolbecker, and W. P. Hetrick, "Cognitive manipulation of brain electric microstates," *NeuroImage*, vol. 146, pp. 533–543, Feb. 2017.

[63] T. A. Suhail, K. P. Indiradevi, E. M. Suhara, S. A. Poovathinal, and A. Ayyappan, "Distinguishing cognitive states using electroencephalography local activation and functional connectivity patterns," *Biomed. Signal Process. Control*, vol. 77, Aug. 2022, Art. no. 103742.

[64] P. S. Muhle-Karbe, J. Jiang, and T. Egner, "Causal evidence for learning-dependent frontal lobe contributions to cognitive control," *J. Neurosci.*, vol. 38, no. 4, pp. 962–973, Jan. 2018.

[65] K. Benchenane, P. H. Tiesinga, and F. P. Battaglia, "Oscillations in the prefrontal cortex: A gateway to memory and attention," *Current Opinion Neurobiol.*, vol. 21, no. 3, pp. 475–485, Jun. 2011.

[66] L. I. Aftanas and S. A. Golocheikine, "Human anterior and frontal midline theta and lower alpha reflect emotionally positive state and internalized attention: High-resolution EEG investigation of meditation," *Neurosci. Lett.*, vol. 310, no. 1, pp. 57–60, Sep. 2001.

[67] H. C. Cromwell, N. Abe, K. C. Barrett, C. Caldwell-Harris, G. H. E. Gendolla, R. Koncz, and P. S. Sachdev, "Mapping the interconnected neural systems underlying motivation and emotion: A key step toward understanding the human affectome," *Neurosci. Biobehav. Rev.*, vol. 113, pp. 204–226, Jun. 2020.

[68] J. W. Y. Kam, R. F. Helfrich, A.-K. Solbakk, T. Endestad, P. G. Larsson, J. J. Lin, and R. T. Knight, "Top–down attentional modulation in human frontal cortex: Differential engagement during external and internal attention," *Cerebral Cortex*, vol. 31, no. 2, pp. 873–883, Jan. 2021.

[69] K. Siuda-Krzywicka, C. Witzel, P. Bartolomeo, and L. Cohen, "Color naming and categorization depend on distinct functional brain networks," *Cerebral Cortex*, vol. 31, no. 2, pp. 1106–1115, Jan. 2021.

[70] I. A. Rosenthal, S. R. Singh, K. L. Hermann, D. Pantazis, and B. R. Conway, "Color space geometry uncovered with magnetoencephalography," *Current Biol.*, vol. 31, no. 3, pp. 515–526, Feb. 2021.

[71] J. Kinnison, S. Padmala, J.-M. Choi, and L. Pessoa, "Network analysis reveals increased integration during emotional and motivational processing," *J. Neurosci.*, vol. 32, no. 24, pp. 8361–8372, Jun. 2012.

[72] A. Gazzaley and A. C. Nobre, "Top-down modulation: Bridging selective attention and working memory," *Trends Cogn. Sci.*, vol. 16, no. 2, pp. 129–135, Feb. 2012.
[73] X. Guo, T. Zhu, C. Wu, Z. Bao, and Y. Liu, "Emotional activity is negatively associated with cognitive load in multimedia learning: A case study with EEG signals," *Frontiers Psychol.*, vol. 13, Jun. 2022, Art. no. 889427.
[74] A. Hillebrand, P. Tewarie, E. van Dellen, M. Yu, E. W. S. Carbo, L. Douw, A. A. Gouw, E. C. W. van Straaten, and C. J. Stam, "Direction of information flow in large-scale resting-state networks is frequency-dependent," *Proc. Nat. Acad. Sci. USA*, vol. 113, no. 14, pp. 3867–3872, Apr. 2016.
[75] A. Woolgar, A. Hampshire, R. Thompson, and J. Duncan, "Adaptive coding of task-relevant information in human frontoparietal cortex," *J. Neurosci.*, vol. 31, no. 41, pp. 14592–14599, Oct. 2011.
[76] R. T. Buxton, A. L. Pearson, C. Allou, K. Fristrup, and G. Wittemyer, "A synthesis of health benefits of natural sounds and their distribution in national parks," *Proc. Nat. Acad. Sci. USA*, vol. 118, no. 14, Apr. 2021, Art. no. e2013097118.
[77] S. C. Van Hedger, H. C. Nusbaum, L. Clohisy, S. M. Jaeggi, M. Buschkuehl, and M. G. Berman, "Of cricket chirps and car horns: The effect of nature sounds on cognitive performance," *Psychonomic Bull. Rev.*, vol. 26, no. 2, pp. 522–530, Apr. 2019.
[78] E. L. Johnson, C. D. Dewar, A.-K. Solbakk, T. Endestad, T. R. Meling, and R. T. Knight, "Bidirectional frontoparietal oscillatory systems support working memory," *Curr. Biol.*, vol. 27, no. 12, pp. 1829–1835.e4, 2017.
[79] J. P. Lachaux, E. Rodriguez, J. Martinerie, and F. J. Varela, "Measuring phase synchrony in brain signals," *Hum. Brain Mapping*, vol. 8, no. 4, pp. 194–208, Jan. 1999.
[80] B. He, L. Astolfi, P. A. Valdés-Sosa, D. Marinazzo, S. O. Palva, C.-G. Bénar, C. M. Michel, and T. Koenig, "Electrophysiological brain connectivity: Theory and implementation," *IEEE Trans. Biomed. Eng.*, vol. 66, no. 7, pp. 2115–2137, Jul. 2019.
[81] K. Mahjoory, V. V. Nikulin, L. Botrel, K. Linkenkaer-Hansen, M. M. Fato, and S. Haufe, "Consistency of EEG source localization and connectivity estimates," *NeuroImage*, vol. 152, pp. 590–601, May 2017.
[82] C. Brunner, M. Billinger, M. Seeber, T. R. Mullen, and S. Makeig, "Volume conduction influences scalp-based connectivity estimates," *Frontiers Comput. Neurosci.*, vol. 10, p. 121, Nov. 2016.
[83] F. Van de Steen, L. Faes, E. Karahan, J. Songsiri, P. A. Valdes-Sosa, and D. Marinazzo, "Critical comments on EEG sensor space dynamical connectivity analysis," *Brain Topogr.*, vol. 32, pp. 643–654, Nov. 2019.

MEEI TYNG CHAI (Member, IEEE) was born in Perak, Malaysia. She received the B.Eng. degree (Hons.) from Universiti Kebangsaan Malaysia, and the M.Sc. and Ph.D. degrees from Universiti Teknologi PETRONAS. She is currently working as an Assistant Professor with Universiti Tunku Abdul Rahman. Her research interests include emotion, human learning and memory assessment using EEG, signal and image processing, machine learning, and deep learning.

TONG BOON TANG (Senior Member, IEEE) was born in Johor, Malaysia. He received the B.Eng. degree (Hons.) and the Ph.D. degree from The University of Edinburgh. He is currently a Professor and the Institute Director of Health and Analytics with Universiti Teknologi PETRONAS. His research interests include biomedical instrumentation, from device and measurement to data fusion. He received the Lab on Chip Award, in 2006, the IET Nanobiotechnology Premium Award, in 2008, the IET Mountbatten Medal, in 2020, and the Top Research Scientists Malaysia, in 2021. He served as the Secretary of the Higher Centre of Excellence (HICoE) Council, and the Chair of the IEEE Circuits and Systems Society Malaysia Chapter. He is also a Chartered Engineer.